INTERNATIONAL JOURNAL OF RESEARCH IN PHARMACY AND CHEMISTRY

Available online at www.ijrpc.com

Research Article

SYNTHESIS, CHARACTERIZATION AND BIOLOGICAL STUDIES OF NOVEL (16Z)-1-ETHYL-1, 4-DIHYDRO-N'-(1-(3, 4- DIHYDRO-6-METHYL-2, 4-DIOXO-2H-PYRAN-3-YL) ETHYLIDENE)-7-METHYL-4-OXO-1, 8-NAPHTHYRIDINE 3- CARBOHYDRAZIDE) AND ITS CU (II), NI (II) AND CO (II) COMPLEXES

Nagula Narsimha, Palreddy Ranjithreddy, Jaheer Mohmed,

Boinala Aparna and CH. Sarala Devi *

Department of Chemistry, University College of Science,
Osmania University, Hyderabad -500007, Telangana, India.

ABSTRACT

Novel (16Z)-1-ethyl-1,4-dihydro-N'-(1-(3,4-dihydro-6-methyl-2,4-dioxo-2H-pyran-3-yl) ethylidene)-7-methyl-4-oxo-1, 8-naphthyridine-3-carbohydrazide) [16Z-EDNEMNC] was prepared. The solid metal complexes of title compound 16Z-EDNEMNC with Cu (II), Ni (II) and Co (II) were isolated and characterized by employing spectro-analytical techniques viz; elemental analysis, ^{1}H-NMR, UV-Vis, IR, Mass, TGA, SEM and spectrophotometry studies. Computational studies were also carried out to know energies and orientation of HOMO and LUMO frontier orbitals of 16Z-EDNEMNC in order to understand the binding modes of metal complexes. The title compound exhibited ditopic property with donor atoms in two directions with Cu (II), resulting in binuclear Cu (II) complex, while Ni (II) and Co (II) showed formation of mononuclear complexes in 1:2 compositions. The DNA cleavage studies were also carried out with title compound and its metal complexes using PBR322 DNA, wherein Cu (II) and Co (II) complexes are proven to act as efficient nucleases in the hydrolytic cleavage of DNA. Docking analysis revealed that two active residue sites of "Thymidine phosphorylase from E.coli" (PDB ID: 4EAF) protein bound with 16Z-EDNEMNC.

Keywords: 16Z –EDNEMNC, Cu (II), Ni (II) and Co (II) metal complexes, binuclear complex.

INTRODUCTION

The Quinolones are family of synthetic broad spectrum antibacterial drugs [1-3]. Quinolone antibacterial drugs have raised much involvement because of their effectiveness and efficiency. The first genesis of Quinolones started with the introduction of 1-ethyl-1, 4-dihydro-7-methyl-4-oxo-1, 8-naphthyridine-3-carboxylic acid [EDMNC] in 1962 for treatment of urinary tract infections [4]. Structure activity relationships (SAR) of the compounds based on EDMNC have contributed to a large group of synthetic bioactive molecules known as Quinolones [5]. EDMNC (1, 8-naphtapyridine derivative) is the first synthetic Quinolone antibiotic. EDMNC is efficient against both gram-negative and gram-positive bacteria [6-9]. It inhibits DNA synthesis by encouraging cleavage of bacterial DNA in the DNA – enzyme complexes of DNA gyrase, resulting in rapid bacterial death [10]. EDMNC hydrazides have wide range of biological activities, namely antibacterial, antifungal [11, 12], anti convulsant [13], anti-inflammatory [14], anti malarial [15] and antituberculosis activities [16]. The present investigation is focused on the synthesis of novel EDMNC based hydrazone using 3-acetyl-6-methyl-3H-pyran-2, 4-dione, and its solid metal complexes with Cu (II), Ni (II) and Co (II). The compound 3-acetyl-6-methyl-3H-pyran-2, 4-dione agent being a chelating agent its metal complexes were already reported and demonstrated for numerous biological applications [17]. As both EDMNC and aforementioned dione are biologically

potential moieties, the resultant title compound of present investigation and corresponding metal complexes were screened for DNA cleavage activity. Further docking studies have been carried out with title hydrazone on the target site of "Thymidine phosphorylase from E.coli" protein.

EXPERIMENTAL

Spectro analytical techniques employed

IR spectra were recorded using Perkin-Elmer 337 Spectrophotometer in KBr pellet in the range 200-4000 cm^{-1}, ^1H -NMR spectra were recorded with Bruker WH (270 MHz) instrument using $CDCl_3$ for ligand, UV-Vis spectra were recorded on Schimadzu UV Spectrophotometer in the wavelength range of
200-800 nm and the mass spectral data were obtained from Electrospray Ionization Mass spectrometry (ESI-MS). Thermal studies were carried out using Shimadzu TGA-50H in nitrogen atmosphere; SEM images were recorded in INCA EDX analyzer. And Polmon apparatus (ModelNo.MP-90) was used to determine melting point. The computational studies were carried out by using HyperChem 7.5 software. The DNA cleavage studies were carried out using Agarose gel electrophoresis. Docking studies were carried out Autodock 4.2 software.

Synthesis

1-ethyl-1, 4-dihydro-7-methyl-4-oxo-1, 8-naphthyridine-3-carbohydrazide (EMNCE) was prepared by employing the following steps [18].

Step–I: Synthesis of Methyl 1-ethyl-1, 4-dihydro-7-methyl-4-oxo-1, 8-naphthyridine-3-carboxylate (MEMNCT)

EDMNC (2g, 8.611mmole) and tetrahydro furan (5oml) were placed in a 100ml round bottom flask and mounted over a magnetic stirrer. Anhydrous potassium carbonate (5.96g, 43.05mmol) was added and the contents were stirred for one hour. Dimethyle sulfate (1.63ml, 12.92mmol) was added to this stirred solution and the mixture was refluxed at 70^0C-80^0C. The progress of the reaction was monitored by TLC using hexane/ethyl acetate (70:30) as the eluent. TLC showed complete disappearance of the starting material after 4 hours and appearance of new spot. After refluxing, the solvent was removed under reduced pressure on a rotary evaporator and the product was extracted with chloroform. The chloroform
Layer was dried over anhydrous sodium sulfate and concentrated under reduced pressure to give MEMNCT.

Step-II: Synthesis of EMNCE

MEMNCT (2g, 8.17mmol) was dissolved in tetrahydro furan (50ml) in a 100ml round bottom flask and $NH_2NH_2.H_2O$ (0.6ml) was added. The contents were refluxed for 3 hours. To the resultant reaction mixture, cold water (50ml) was added and stirred for 15 min. A solid separated out was filtered at pump and dried.

Step –III: Synthesis of 16Z –EDNEMNC

To a stirred solution of EMNCE (0.01mole) in methanol (20 ml), 3-acetyle-6-methyl-3H-pyran-2, 4-dione (0.01mole) was added. A few drops of conc. sulfuric acid was added and the solution was refluxed on an oil bath for 2-3 hrs at 60-80 ^{0}C. After completion of the reaction, monitored by TLC the precipitated white solid was filtered, thoroughly washed with hot methanol and dried. (Yield 85%, m. p 280^0C), the synthetic path for the 16Z –EDNEMNC shown in scheme: 1 below.

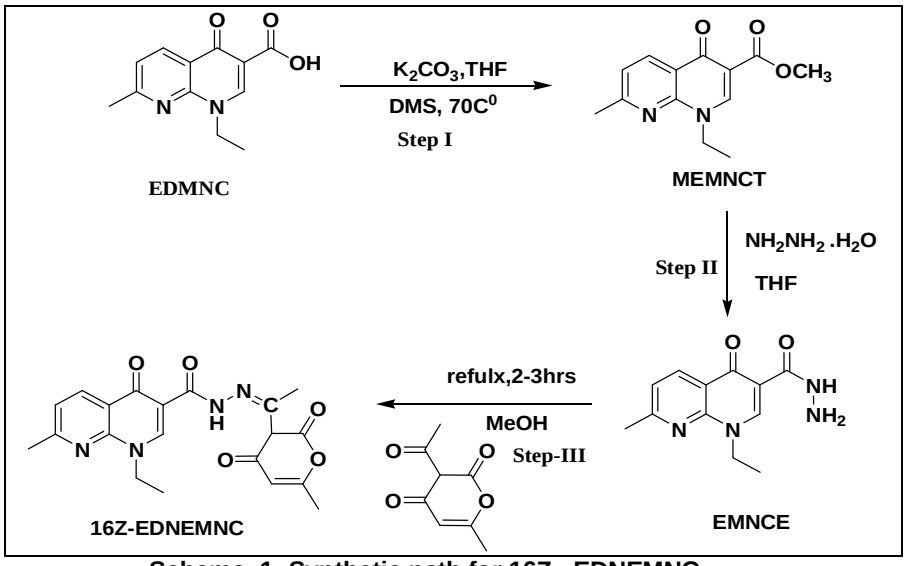

Scheme. 1: Synthetic path for 16Z –EDNEMNC

Synthesis of metal complexes of 16Z –EDNEMNC

The complexes were prepared by refluxing the mixture of ligand 16Z –EDNEMNC in chloroform and metal salts in methanol (1:2 mole) for 15-18 hours at 80-90^{0}C by adjusting pH in the range 6-7 for complex formation (scheme:2). The resulting solutions were concentrated and cooled. On cooling colored precipitate is obtained, which is filtered, washed several times with chloroform, methanol and dried. It is stored in a desiccator over anhydrous $CaCl_2$. All the complexes are stable to air and moisture.

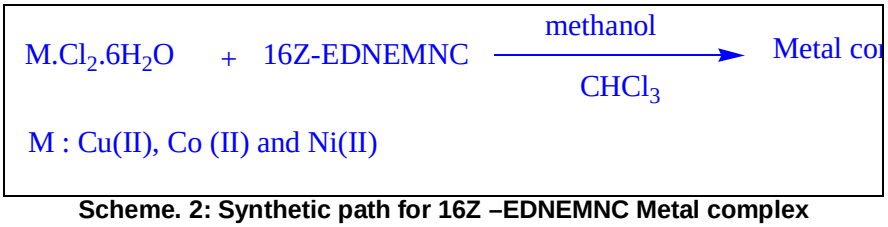

Scheme. 2: Synthetic path for 16Z –EDNEMNC Metal complex

RESULTS AND DISCUSSION

Spectral studies of 16Z –EDNEMNC

Mass spectrum

The mass spectrum of ligand 16Z –EDNEMNC exhibited (figure: 1) peak at m/z 397 representing [M+1] peak, along with peak at m/z 419 corresponding to sodium adduct peak [M+23].

^{1}H NMR Spectrum

The ^{1}H- NMR spectrum of ligand 16Z –EDNEMNC shows (figure: 2) the signals at δ 8.42ppm (s, 1H, H-2-napthyridine), δ 8.82ppm (d, 1H, H-5-napthyridine) and δ 7.37ppm (d, 1H, H-6-napthyridine). The amide proton signal is recorded at δ 13.25ppm (s, 1H, NH) [18]. The signals at δ 5.6 ppm (s,1H) and δ 3.6 ppm (s,1H) corresponds to HC = C proton and CH proton adjacent to lactone respectively. The other peaks observed correspond to chemical shifts of corresponding protons viz; δ 4.60 ppm (q, 2H, N-CH_2), δ 1.62 ppm (t,3H, N-CH_2 $\underline{CH_3}$), δ 2.21 ppm (s,3H, 7-$\underline{CH_3}$) and the singlet at δ 2.8 -3.2 ppm (pyran ring CH_3).

IR spectrum

The IR spectrum displayed (figure: 3) bands at 1653cm^{-1} and 1676 cm^{-1} corresponding to the stretching frequencies of v C=O (pyran ring), 1682 cm^{-1} and 1609 cm^{-1} characteristic bands of v (C=O) (Quinolone ring), the strong band at 1521cm^{-1} is attributable to v (C=N) vibrations, 3078cm^{-1} (aromatic –CH) and 1496 cm^{-1} (C=C).

Electronic spectral data

The UV spectrum shows (figure: 4) two peaks at wavelengths 41666 cm^{-1} and 29239 cm^{-1} attributable to n→ π* (C=O) and π→ π* (C=C) transitions respectively.

Computational Studies of 16Z - EDNEMNC

As the quantum chemical calculations enable to understand donor and acceptor properties of molecules, in the present investigation the HyperChem 7.5 software was used for quantum mechanical calculations. The geometry optimization, contour maps of highest occupied molecular orbitals (HOMO) and lowest unoccupied molecular orbitals (LUMO) and corresponding binding energy values were computed using semi empirical single point PM3 method (figure: 5(a), 5(b),5(c),5(d)and 5(e)). From binding energy values it is evident that the ionized form with relatively lower value can readily donate electrons than neutral form of 16Z –EDNEMNC. The energy difference in HOMO and LUMO levels is less in ionized form indicating more reactivity and its ability to bind with metal ion.

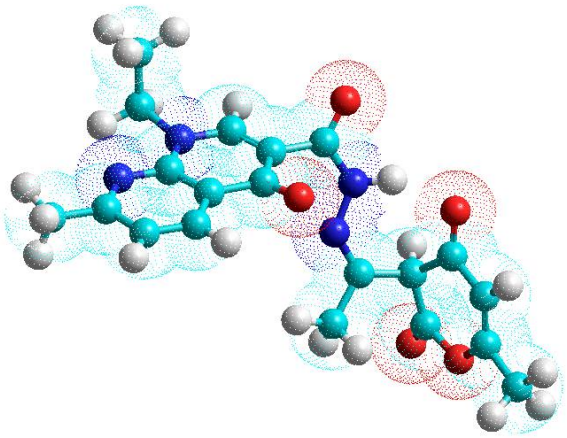

Fig. 5 (a): Geometry Optimized Structure of 16Z –EDNEMNC neutral form

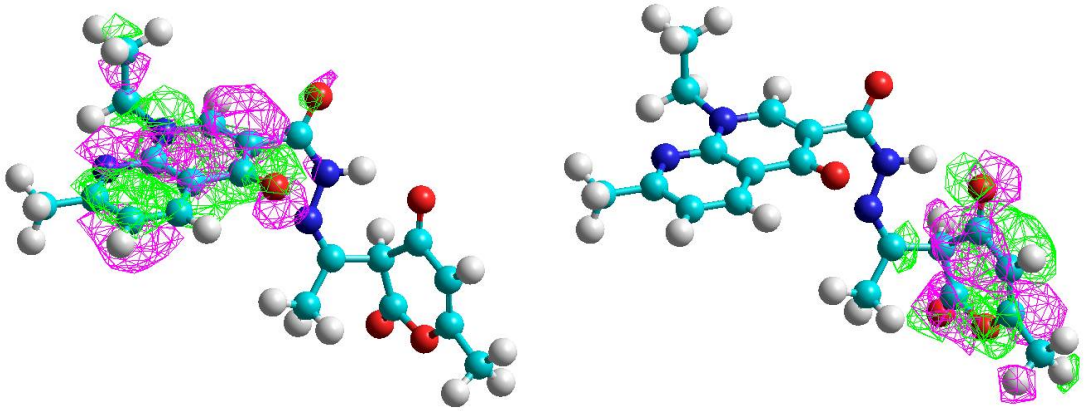

HOMO (Binding Energy: - 8.805eV) **LUMO (Binding Energy: -0.927eV)**

Fig. 5(b): The contour maps of highest occupied molecular orbitals and lowest unoccupied molecular orbitals of 16Z –EDNEMNC neutral form

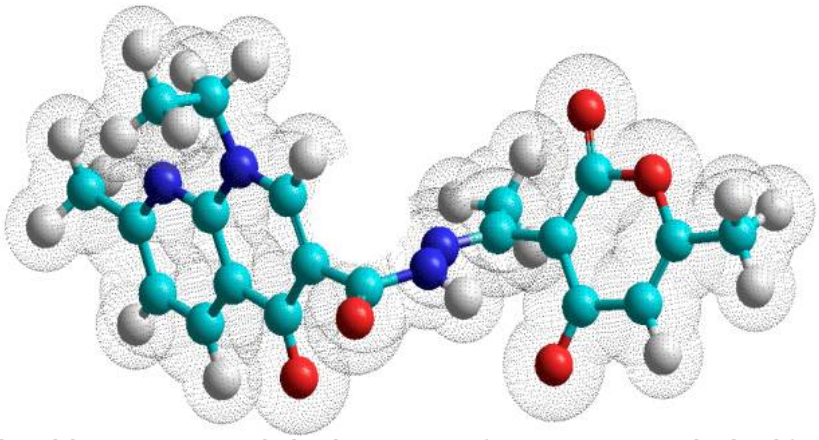

Fig. 5(c): Geometry Optimized Structure of 16Z –EDNEMNC ionized form

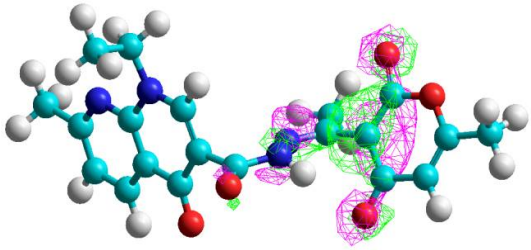

HOMO (Binding Energy: -4.519eV)

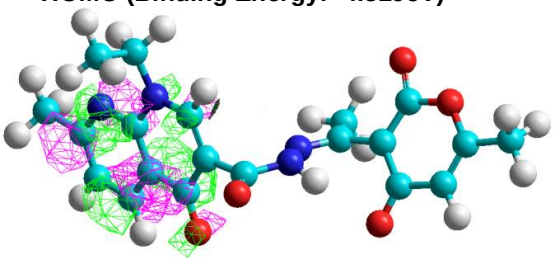

LUMO (Binding Energy: 1.448eV)

Fig. 5(d): The contour maps of highest occupied molecular orbitals and lowest unoccupied molecular orbitals of ionized form of 16Z –EDNEMNC

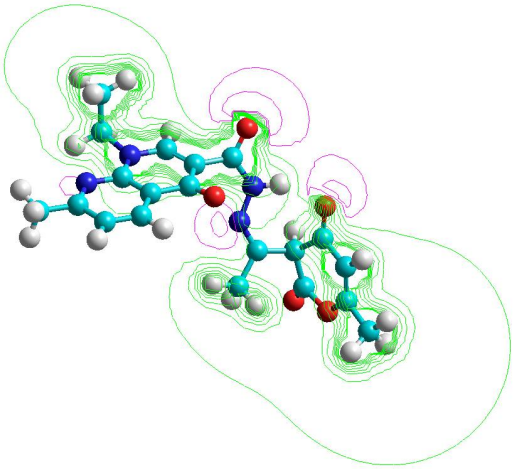

Molecular Form

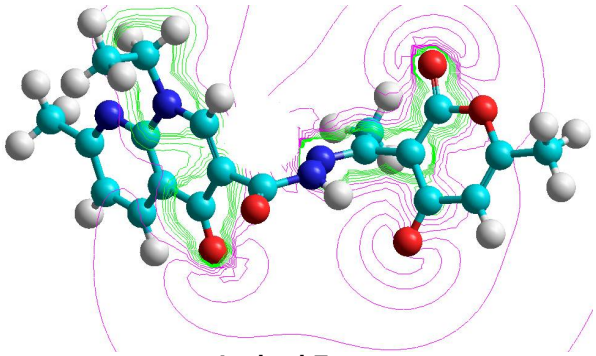

Ionized Form

Fig. 5(e): Contour maps of electrostatic potentials of molecular and ionic forms of 16Z –EDNEMNC

The contour maps of electrostatic potentials in figure: 5(e) indicates the charge delocalization on nitrogen and oxygen sites between molecular and ionized forms.

Spectrophotometric studies

An attempt is made to establish the stoichiometric metal to ligand ratio of the complexes formed from Co (II) – 16Z-EDNEMNC and Ni (II) -16Z –EDNEMNC using job's method and mole –ratio method.

Mole-ratio method

A series of solutions are prepared [19] such that, the molar concentration of the metal ion is held constant and while that of the 16Z –EDNEMNC is varied [20]. The pH of the solution is maintained at 10 by adding buffer. A graph is plotted between absorbance and mole-ratio of the ligand. Two straight lines of different slopes are obtained. The intersection of the two lines occurs at a point corresponding to their combination in the complex (figure: 6, 7).

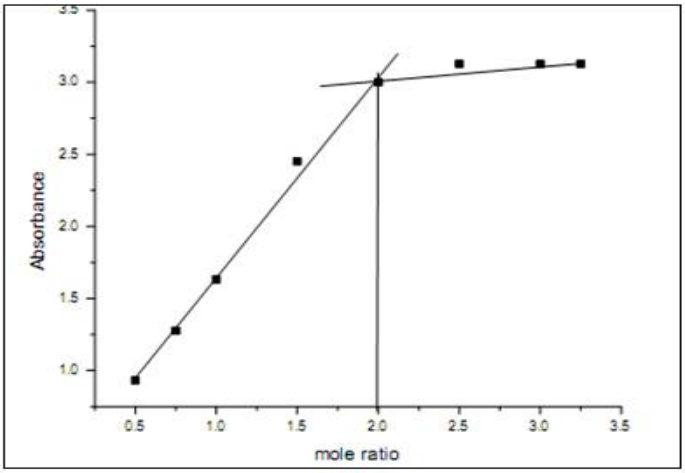

Fig. 6: Plot of absorbance versus mole ratio of ligand at 303 K in ethanol medium (Co (II) – 16Z-EDNEMNC ($\lambda max_{=}$ 378 nm))

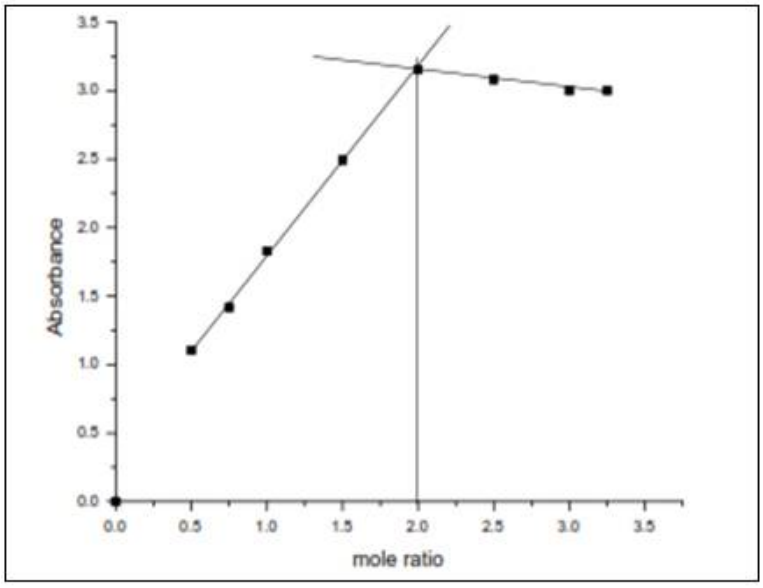

Fig. 7: Plot of absorbance versus mole ratio of ligand at 303 K in ethanol medium (Ni (II)-16Z –EDNEMNC (λmax =380))

Job's continuous variation method

In this method, the solutions of Ni (II) and 16Z –EDNEMNC with identical concentrations are mixed in different volume ratios, keeping total volume of the mixture constant. The pH of the solution was maintained at 10 by adding buffer and the absorbance of each solution was measured at a wavelength 420 nm (λmax). A graph is plotted between absorbance and mole fraction of the ligand. The graph showed (figure: 8) a maximum absorbance value at 0.67 mole fraction of the ligand confirming 1:2 stoichiometric composition of metal ligand in complex.

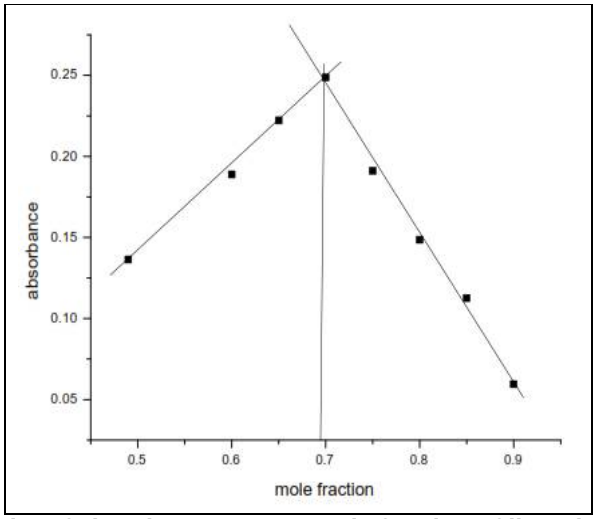

Fig. 8: Plot of absorbance versus mole fraction of ligand at 303 K in ethanol medium (Ni (II) – 16Z –EDNEMNC (λmax=420))

Both the methods suggest 1:2 metal to ligand ratio in Co (II) and Ni (II) metal complexes.

Characterization of metal complexes of 16Z –EDNEMNC

Mass spectrum of Cu (II) -16Z –EDNEMNC

The mass spectrum showed (figure: 9) peak at m/z 700 corresponding to the [M+4H] ion peak, which indicates the formation of metal complex in 1:1 mole ratio (M: L).

Mass spectrum of Co (II) – 16Z –EDNEMNC

The mass spectrum of Co (II) – 16Z –EDNEMNC shows (figure: 10) a base peak at m/z 849, which is in accordance with the expected molecular ion peak. From the mass spectrum it is clear that 1:2 mole ratio (M: L) of metal complex is formed.

Mass spectrum of Ni (II) – 16Z –EDNEMNC

The mass spectrum displays (figure: 11) peak at m/z 849 corresponding to the molecular ion peak, indicating the formation of metal complex in 1:2 mole ratio (M: L).

IR Spectra

In order to study the binding mode of the ligand to the metal complexes, the IR spectrum of the ligand (16Z –EDNEMNC) is compared with the IR spectra of its metal complexes. All the metal complexes (figure: 12 (a), 12 (b) &12(c) show down shifting in v (C=N) compared to their respective ligand (16Z – EDNEMNC), these suggest that the nitrogen atom of the -C=N (azomethine) has participated in the coordination. The stretching frequency of v C=O (pyran), is shifted to lower frequency which indicates the participation of carbonyl oxygen in bonding with metal ion. All the metal complexes show a broad band around 3340cm^{-1} -3450cm^{-1} indicating the presence of coordinated water molecule, The stretching frequency of v C=O (Quinolone ring) shifted to 1692cm^{-1} confirms the participation of carbonyl oxygen in bonding with Cu(II). These suggest that Cu (II)-16Z-EDMENC act as a binuclear complex. The IR spectrum of the metal complexes also show some new bands in the region 490-420 $cm^{-1}$and 550-520cm^{-1} which are assigned to v (M-N) and v (M-O) bands respectively. The IR spectral data are shown in table: 1.

Electronic spectral data

The electronic spectrum of the metal complexes (figure: 13a, 13b) were compared with the free ligand. The complexes of Cu (II) and Co (II) show bands in the region 18181 cm^{-1} - 17391 cm^{-1}, 14044 cm^{-1} - 12578 cm^{-1} respectively, which can be assigned to d-d transitions of metal complexes in respective systems.

SEM & EDX

Scanning electron microscopy (SEM) is used to evaluate surface morphology and particle size of the free ligand and its Cu (II), Ni (II) and Co (II) complexes. The SEM image of 16Z –EDNEMNC shows (figure: 14) a tube like shape with 2µm particle size. While a cauliflower like structure is observed in Cu (II) complex (figure: 15) with particle size 2µm, an ice rock like shape in Co (II) complex (figure:16) with particle size of 2µm and Ni (II) complex shows twisted fiber morphologies in the form of a bundle with particle size 2µm (figure:17). It is inferred from pictographs that there is different and characteristic morphology for the synthesized complexes. The elemental composition of the ligand and its metal complexes obtained from the EDX data (Table: 2) are in good agreement with the predicted mass and theoretical composition of the same.

Thermal analysis

The thermal stability behaviors of metal complexes were studied by thermo gravimetric analysis (TGA).

TGA curve of Cu (II) – 16Z –EDNEMNC presented in figure: 18 reveals the weight loss from 110^{0}C to 160^{0}C corresponding to loss of coordinated water molecules. The steep change of weight loss between 181^{0}C to 273^{0}C signifies the partial decomposition of ligand moiety. The total decomposition of ligand moiety is observed between 366^{0}C to 658^{0}C, which is accompanied by an exothermic peak in DTA curve. In the DTA curve corresponding exothermic peak is observed between 123^{0}C to 273^{0}C which supports the loss observed on TGA. Above 766^{0}C the decrease of weight corresponds to loss of total organic moiety leaving residue of stable metal oxide. The exothermic peak in DTA curve infers pyrolytic nature ascribable to presence of more number of nitrogen atoms in ligand moiety.

Thermogram of Co (II)-16Z –EDNEMNC shows decomposition (figure: 19) in the region 160^{0}C-220^{0}C where an exothermic peak at 180^{0}C on DTA corresponds to the loss of coordinated water molecules. The weight loss between 220^{0}C -460^{0}C, corresponds to the decomposition of Ligand moiety which is also indicated by an exothermic peak at 440^{0}C on DTA curve. The final residue represents the formation of stable metal oxide. An endothermic peak on DTA which is probably due to phase

transition corresponds to the melting of cobalt. All the TGA results were in good agreement with the composition of the metal complexes.
Based on the above interpretation the following tentative structures can be assigned for the metal complexes synthesized.

Tentative structures of metal complexes

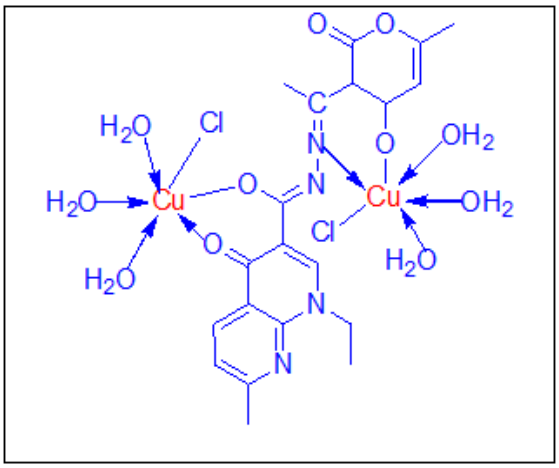

Fig. 20(a): Structure of binuclear Cu (II) – 16Z –EDNEMNC

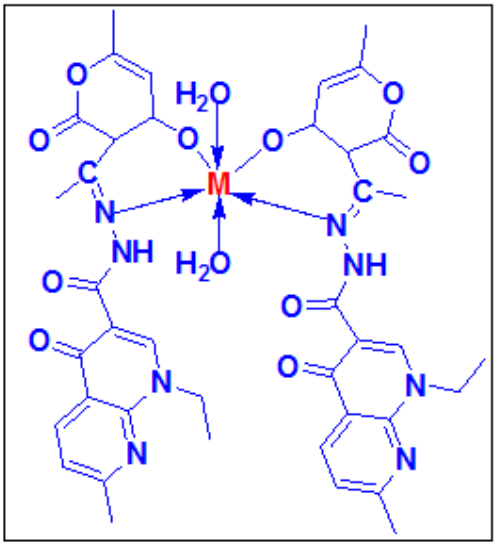

Fig. 20(b): Structures of M (II) – 16Z –EDNEMNC Where M: Co (II) and Ni (II)

DNA cleavage studies

Agarose gel electrophoresis is a successful method in studying DNA cleavage by the potential compounds. DNA is an important substrate for the hydrolytic cleavage because of its poly anionic nature. For the DNA cleavage analysis a potency of compounds are quantitatively evaluated on super coiled plasmid PBR322 in the absence of oxidizing or reducing agents. In the present study the candidate compound 16Z –EDNEMNC and its metal complexes have been tested for DNA cleavage activity. The experimental result (figure: 21) indicates hydrolytic DNA cleavage in presence of Cu (II)-16Z –EDNEMNC and Co (II)-16Z –EDNEMNC complexes wherein super coiled DNA (form I) is converted into nicked form DNA (form II). While no such activity is observed with 16Z –EDNEMNC and Ni (II)-16Z –EDNEMNC complex. It is also evident from these studies that the DNA cleavage activity increases with enhanced concentration of metal complex.

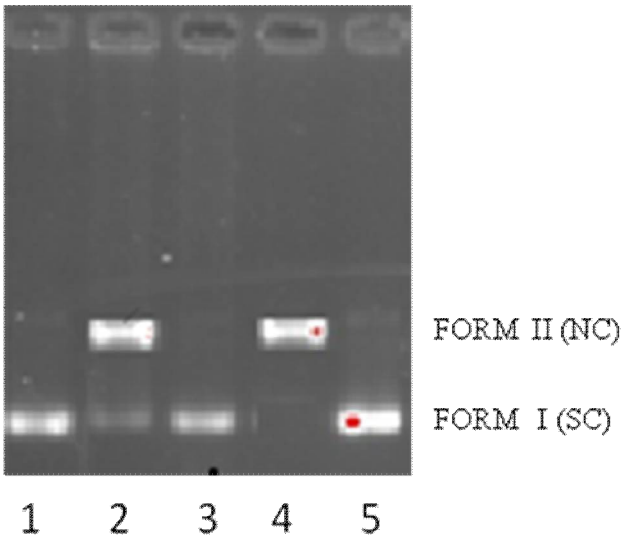

Fig. 21: DNA cleavage studies on 16Z –EDNEMNC, Cu (II) - 16Z–EDNEMNC, Co (II) - 16Z –EDNEMNC and Ni (II) - 16Z –EDNEMNC
Lane 1: DNA marker (1µl+4 µl Tris – HCl Buffer) Lane 2: DNA (1 µl+4 µl Tris – HCl Buffer) + Co (II)- 16Z –EDNEMNC (5 µl of 2 mg/ml) Lane 3: DNA (1 µl+4 µl Tris – HCl Buffer) + Nl (II)- 16Z – EDNEMNC (5 µl of 2 mg/ml) Lane 4: DNA (1 µl+4 µl Tris – HCl Buffer) + Cu (II)- 16Z –EDNEMNC (5 µl of 2 mg/ml) Lane 5: DNA (1 µl+4 µl Tris – HCl Buffer) + 16Z –EDNEMNC (5 µl of 2 mg/ml)

Docking studies

Molecular docking studies were performed to elucidate the binding mode of 16Z –EDNEMNC against "Thymidine phosphorylase from E.coli" (PDB ID: 4EAF) protein with 1.55 Å resolution (figure: 22). In the present study we performed docking to locate the appropriate binding orientations and conformations of various inhibitors in the binding pocket using the Graphical User Interface program "Auto-Dock". Auto Dock is an automatic docking tool designed to predict how small molecules bind to a receptor of known 3D structures, which generates grids and calculates the dock score to evaluate the conformers. Kollman united atom charges, solvation parameters and polar hydrogen's were added to the receptor for the preparation of protein in docking simulation, Gasteiger- Huckel charges were assigned and then non-polar hydrogens were merged as the docking ligands are not peptides. All torsions were allowed to rotate during docking. Binding pose with the lowest docked energy belonging to the top-ranked cluster was selected as the final model for post-docking analysis with AutoDock Tools. Results obtained from AutoDock provided pertinent information on the binding orientation of ligand-receptor interactions. The free energies of binding (ΔGb) calculated by AutoDock programme are summarized in table: 3.

Docking Results: In silico Molecular docking of (16Z –EDNEMNC) for 4EAF inhibition

Molecular docking studies are commonly used for predicting binding modes and energies of protein-ligand interactions [21]. Molecular Docking was accomplished using Autodock 4.2 which is a suite of automated docking tools, was used to predict the affinity, activity, binding orientation of 16Z –EDNEMNC on the target protein "Thymidine phosphorylase from E.coli". Binding analysis was based on free energy of binding, lowest docked energy and calculated RMSD values. 16Z –EDNEMNC was found to bind at active site of 4EAF with lowest binding energy of -7.85 Kcal/Mol. Docking analysis of 4EAF with 16Z- EDNEMNC enabled us to identify specific residues viz. Thr-123, Gln-156 within 4EAF binding pocket to play an important role in ligand binding affinity.

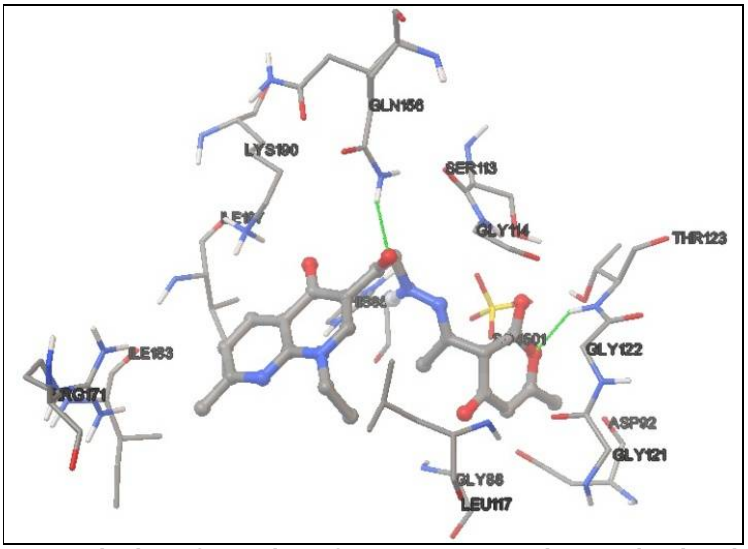

Fig. 22: Docked conformation of 16Z –EDNEMNC in protein Thymidine phosphorylase from E.coli (PDB ID: 4EAF) (colored by atom: carbon- grey; nitrogen-blue; oxygen-red) hydrogen bonds are indicated as green lines

Table 3: Molecular docking result with" Thymidine phosphorylase from E.coli" (PDB ID: 4EAF) protein

Compound Name	Name of the source protein	Interacting amino acids	Grid X-Y-Z coordinates	Binding energy ΔG (Kcal/Mol)
16Z-EDNEMNC	Thymidine phosphorylase from E.coli (PDB ID: 4EAF)	Thr-123, Gln-156	55.411, 28.471, 21.961.	-7.85

CONCLUSIONS

Novel EDMNC based hydrazone and its Cu (II), Ni (II) and Co (II) complexes were prepared and characterized by various physico-chemical techniques viz; elemental analysis, ^{1}H-NMR, UV-Vis, IR, Mass, TGA and SEM. All the metal complexes were formed in 1:2 molar ratios; except Cu (II) metal. 16Z-EDNEMNC was found to bind at Thr-123, Gln-156 active sites within 4EAF protein with lowest binding energy value of -7.85Kcal/Mole, which indicates that 16Z-EDNEMNC has binding affinity to inhibit 4EAF. DNA hydrolytic cleavage is more pronounced in the presence of Cu (II) – 16Z – EDNEMNC and Co (II) – 16Z –EDNEMNC.

ACKNOWLEDGMENTS

Authors (NN and CHS) are thankful to Department of Chemistry and Instrumentation Lab Facilities, Osmania University for providing necessary facilities, the Central Facilities for Research & Development (CFRD), and Department of Microbiology, Osmania University for providing necessary facilities. NN (SRF) is thankful to UGC for the award of Senior Research Fellowship.

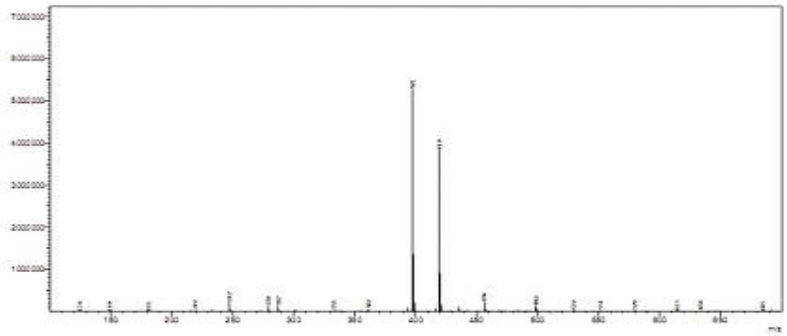

Fig. 1: Mass spectrum of 16Z –EDNEMNC

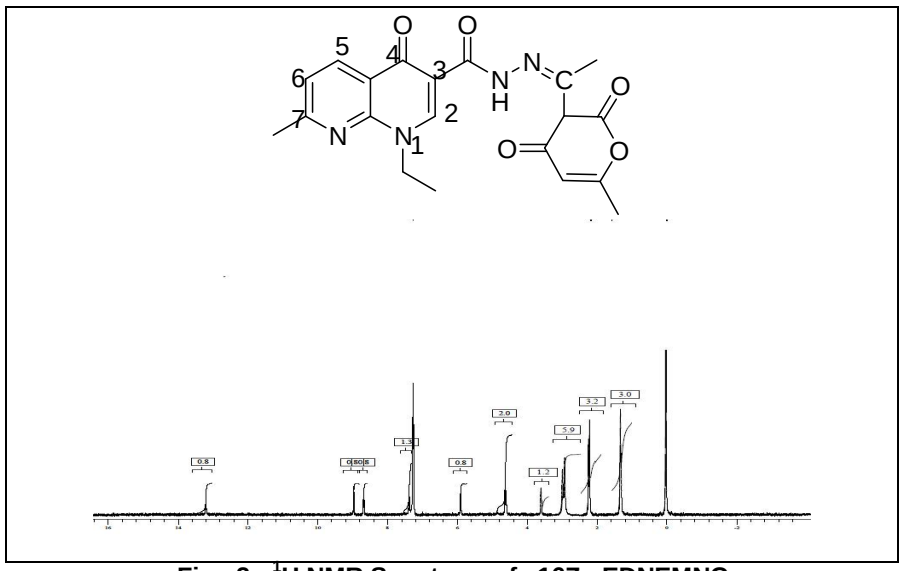

Fig. 2: ^{1}H NMR Spectrum of 16Z –EDNEMNC

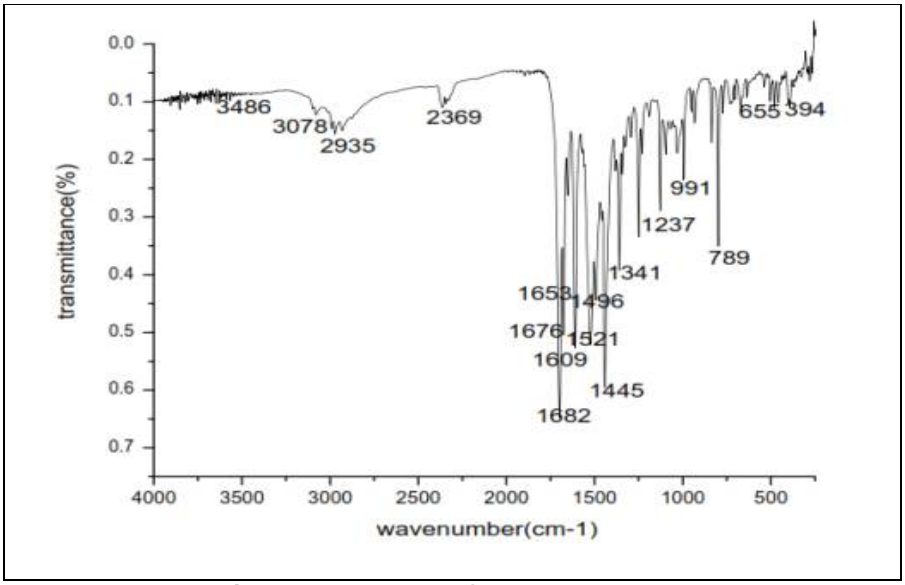

Fig. 3: IR spectrum of 16Z –EDNEMNC

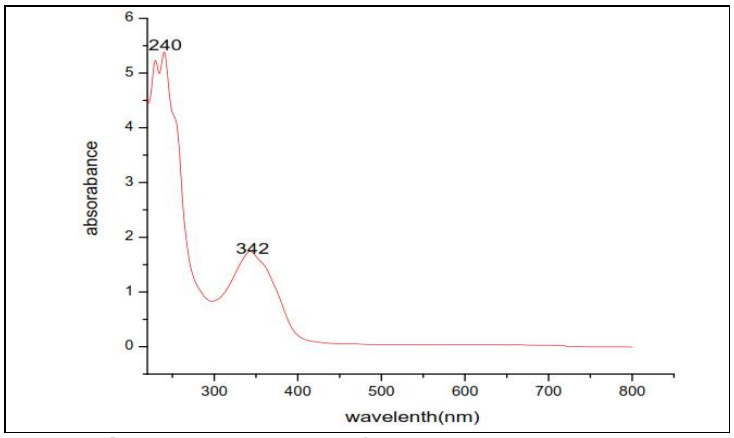

Fig. 4: UV spectrum of 16Z –EDNEMNC

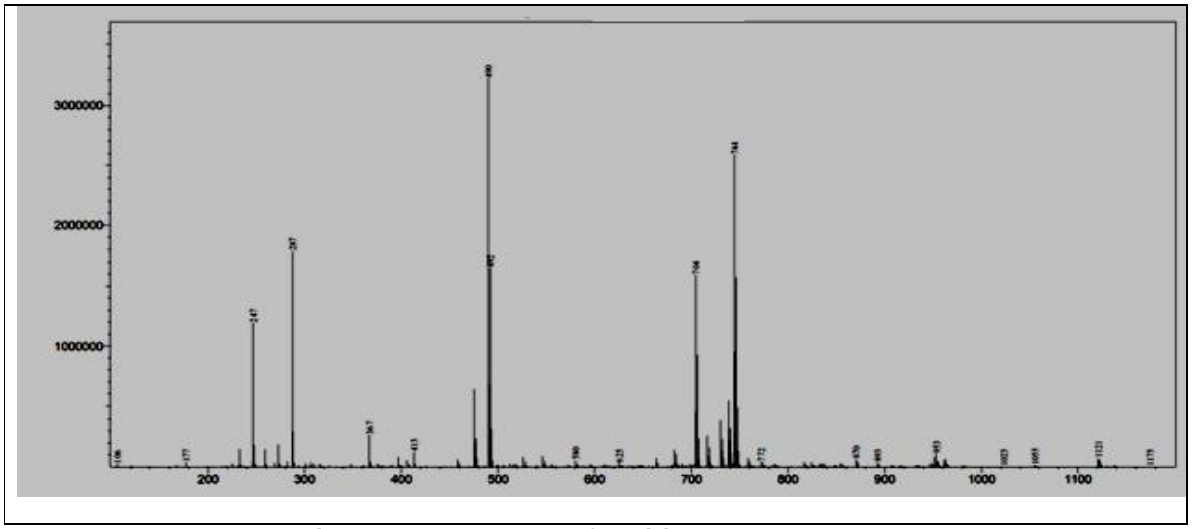

Fig. 9: Mass spectrum of Cu (II) – 16Z –EDNEMNC

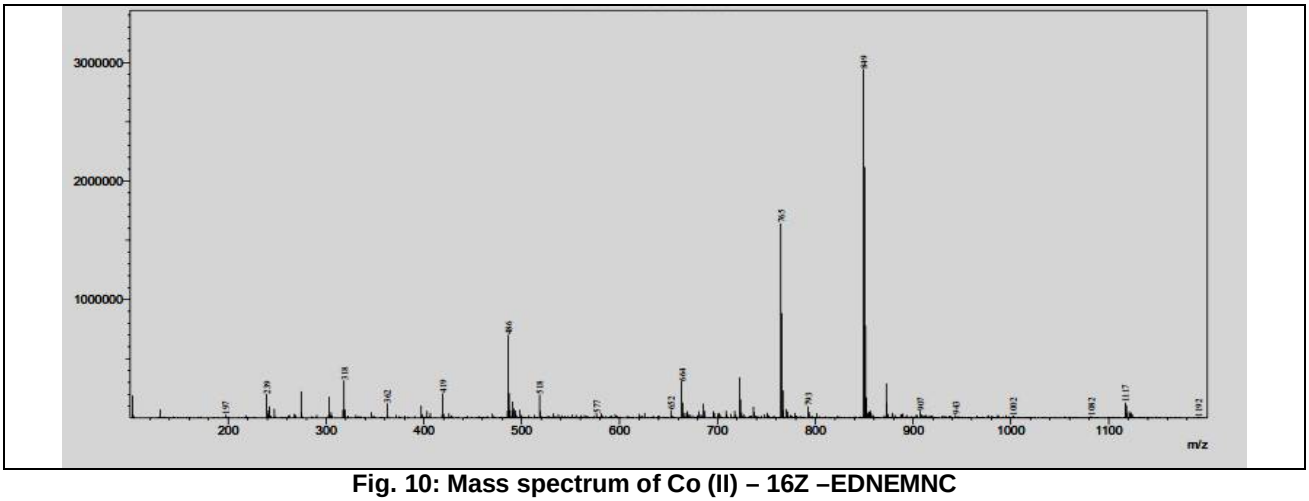

Fig. 10: Mass spectrum of Co (II) – 16Z –EDNEMNC

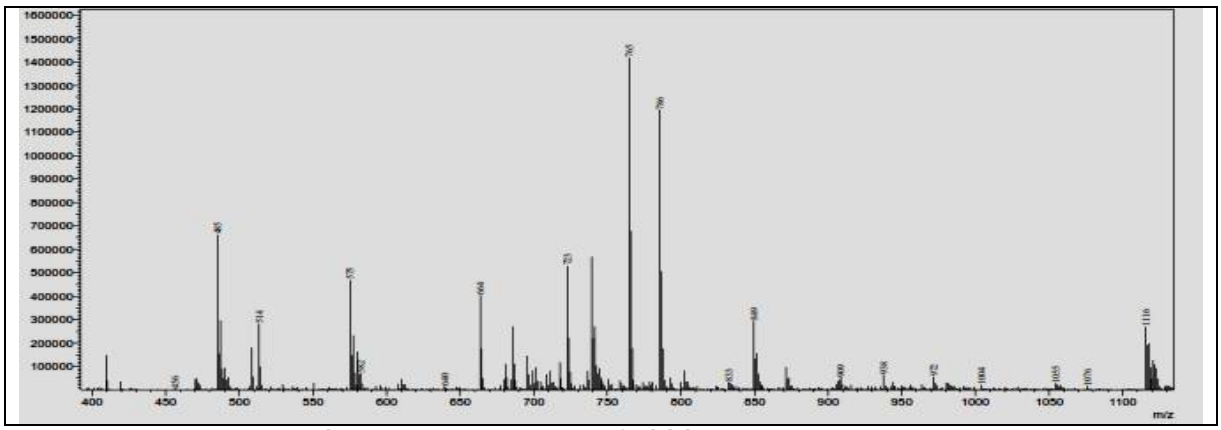

Fig. 11: Mass spectrum of Ni (II) – 16Z –EDNEMNC

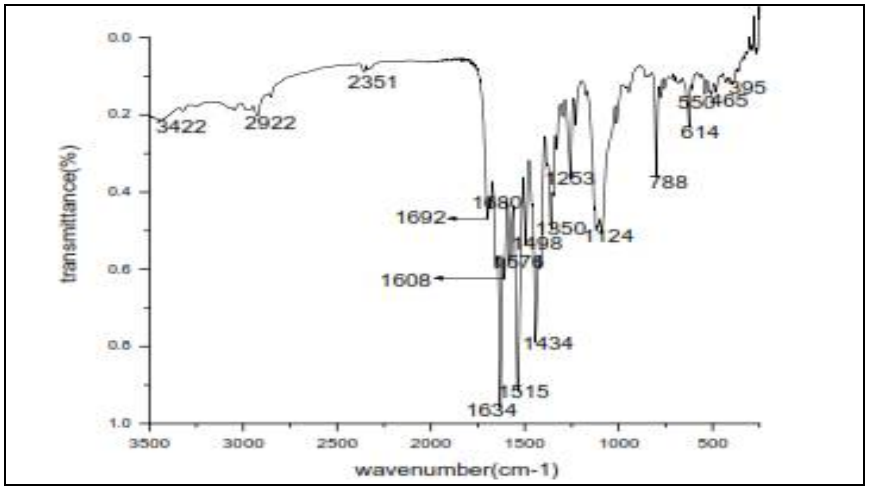

Fig. 12 (a): IR spectrum of Cu (II) – 16Z –EDNEMNC

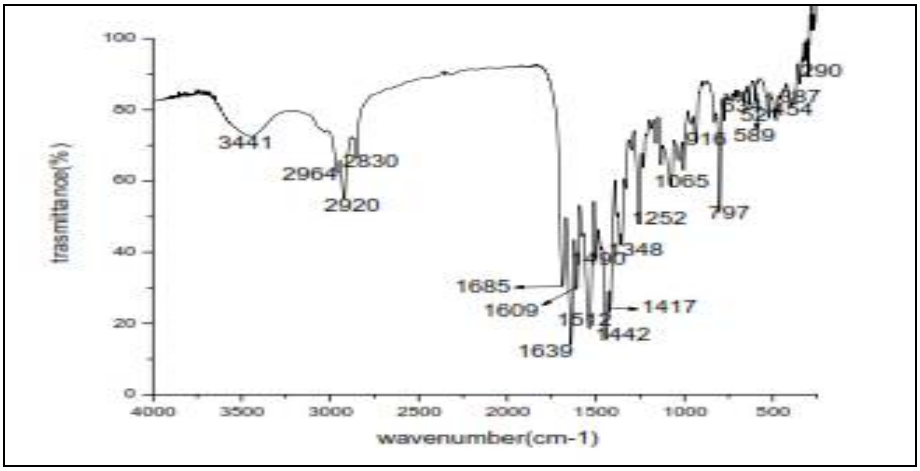

Fig. 12(b): IR spetrum of Co (II) – 16Z –EDNEMNC

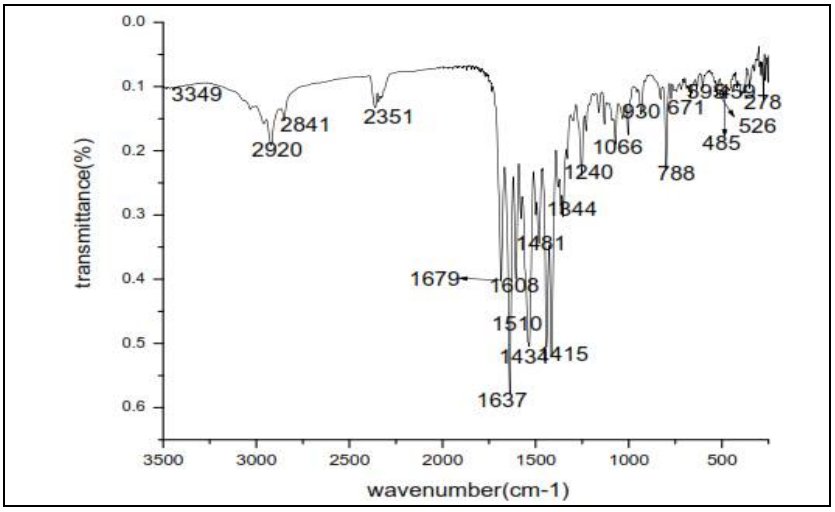

Fig. 12(c): IR spetrum of Ni (II) – 16Z –EDNEMNC

Table 1: FT-IR data of the 16Z –EDNEMNC and its metal complexes

Compound	v C=N cm^{-1}	v C=O (pyran) cm^{-1}	v (M-O) cm^{-1}	v (M-N) cm^{-1}
16Z –EDNEMNC	1521	1653	-	-
Cu (II) – 16Z –EDNEMNC	1515	1634	550	465
Co (II)-16Z –EDNEMNC	1512	1639	535	487
Ni (II)-16Z –EDNEMNC	1510	1637	520	485

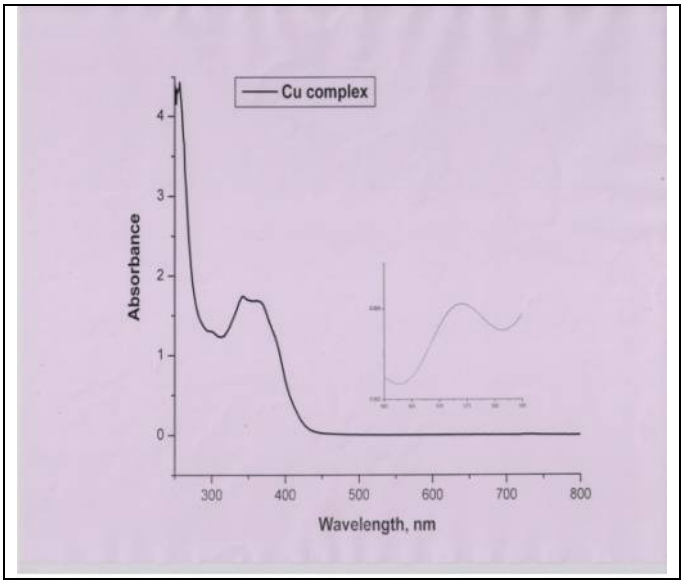

Fig. 13(a): Electronic spectrum of Cu (II)-16Z –EDNEMNC

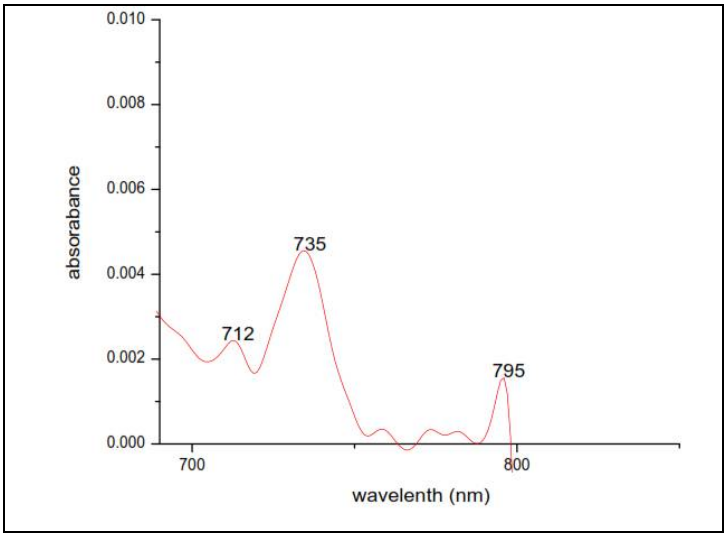

Fig. 13(b): Electronic spectrum of Co (II)-16Z –EDNEMNC

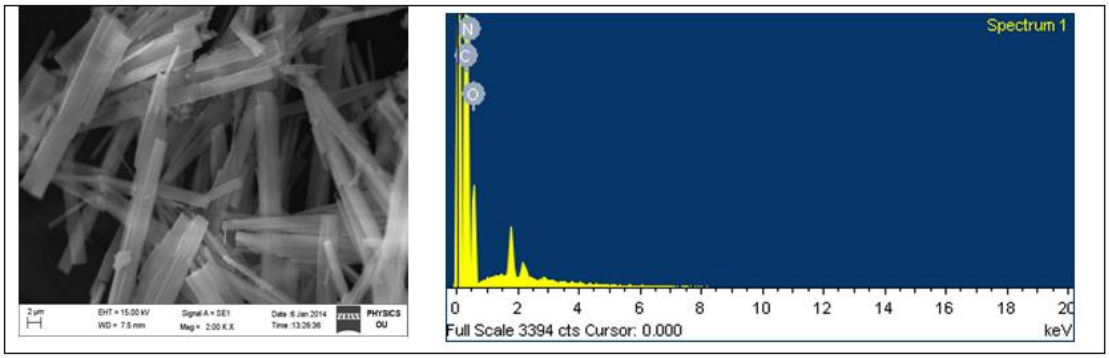

Fig. 14: Scanning electron microscope & EDX images 16Z –EDNEMNC

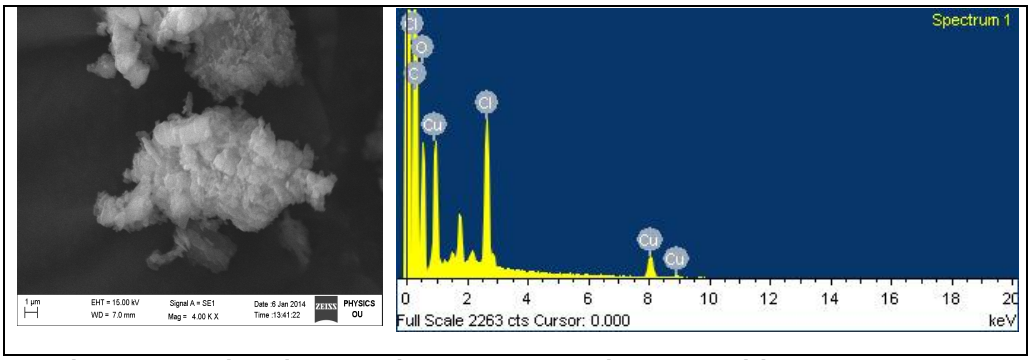

Fig. 15: Scanning electron microscope & EDX images Cu (II) -16Z –EDNEMNC

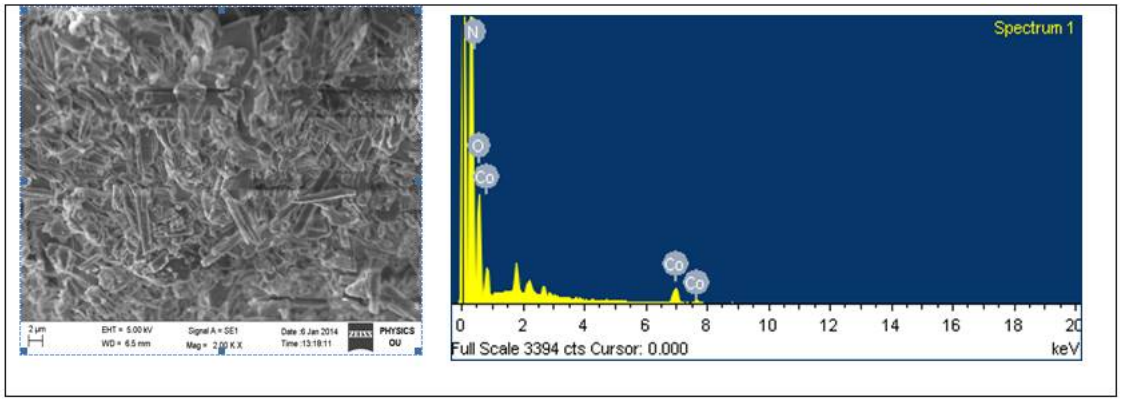

Fig. 16: Scanning electron microscope & EDX images Co (II) -16Z –EDNEMNC

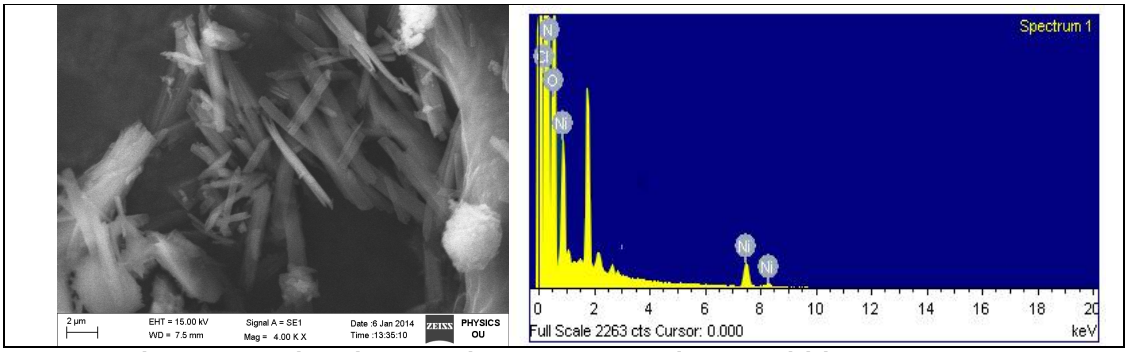

Fig. 17: Scanning electron microscope & EDX images Ni (II) -16Z –EDNEMNC

Table 2: Physical constants and Energy dispersive X-ray Spectroscopy (EDX) data

Compound	Molecular Formula	M.pt	Analysis found (calc) %				
			C	N	O	Cl	Metal
16Z –EDNEMNC	$C_{20}O_5N_4H_{20}$	280^{0}C	56.60 (60.60)	18.11 (14.14)	25.30 (20.20)	- -	-
Cu (II) – 16Z -EDNEMNC	$Cu_2C_{20}O_{11}N_4H_{30}Cl_2$	> 350^{0}C	58.89 (34.20)	14.31 (8.0)	22.03 (25.14)	7.21 (10.14)	11.87 (18.0)
Co (II) – 16Z–EDNEMNC	$CoC_{40}O_{10}N_8H_{38}$	> 400^{0}C	53.92 (56.50)	14.90 (13.19)	24.30 (18.80)	- -	6.29 (6.94)
Ni (II) – 16Z –EDNEMNC	Ni $C_{40}O_{10}N_8H_{38}$	> 400^{0}C	57.92 56.50)	13.20 (13.19)	23.32 (18.80)	- -	5.32 (6.91)

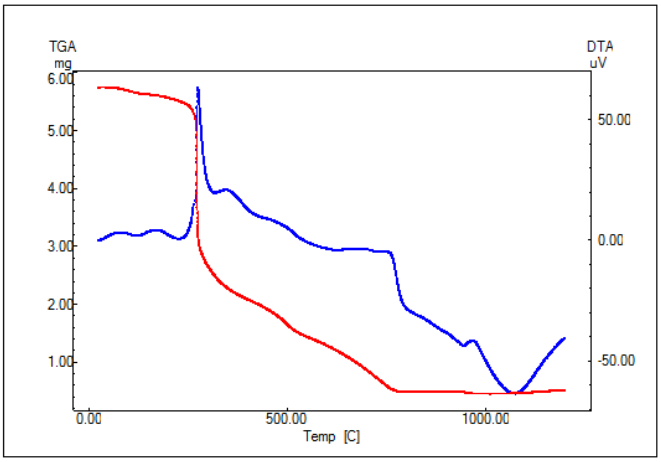

Fig. 18: Thermogram of Cu (II) – 16Z –EDNEMNC

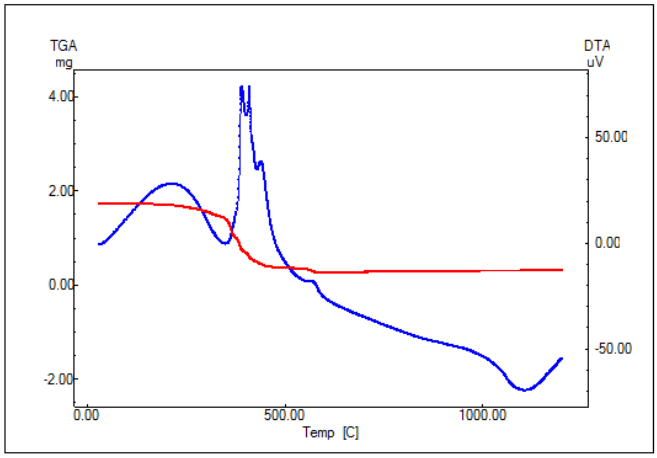

Fig. 19: Thermogram of Co (II) – 16Z –EDNEMNC

REFERENCES

1. Andriole VT. The Quinolone Academic Press. 1989.
2. Andersson MI and Macgown AP. Development of the quinolones. J.Antimicrob.Chemother. 2003; 51: 1-11.
3. Ivanov DV and Budanov SV. Ciprofloxacin and antibacterial therapy of respiratory tract infections Antibiot. Khimioter. 2006;51(5):29-37.
4. Sanofi-aventis U.S.LLC. NegGram Caplets (Nalidixic acid .USP). 2008.
5. Gaurav G, Suvarna and kini G. Synthesis and evaluation of new quinazolone derivative of nalidixicacid as potential bacterial and antifngala agents. Eur J Med Chem. 2006;41:256-262.
6. Schaumann R and Rodloff AC. Activites of quinolones against obligate anaerobic bacteria. Anti –Infective Agents. Med Chem. 2007;6:49-56.
7. Shen LL and Chu DTW. Type DNA topoisomerases as antibacterial targets. Current pharmaceutical Design. 1996;2:195-208.
8. Peterson LR. Quinolone molecular structure-activity relationship: improving antimicrobial activity. Clin. Infect. Dis. 2001;33:80.
9. Des Clin Infect. Dis.1996;2:195.
10. Pedrini AM, Geroldi D, Siccardi A and Falaschi. Studies on the mode of action of nalidixic acid. Eur AJ. Biochem. 1972 25:359-365.
11. Kamel AM, Lobna MA, El-Sayed ML, Mohamed IH and Raina HB. Hydrazones of 2-aryl-quinoline-4-carboxylicacid hydrazides: synthesis and preliminary evalution as a antimicrobial agents. Bio.Med.chem. 2006;14:8675-8682.
12. Ozdemir A, Turan-zitouni G, Kaplancikl ZA, Demirci F and Iscan G. Studies on hydrazone derivivaties anti fungalagents. Med Chem. 2008;23: 470-475.
13. Dimmock JR, Vashisha SC and Stables JP. Anti convulsant properties of various acetyl hydrazones, oxamoylhydrazones and semicarbazones derived from aromatic and unsaturated carbonyl compounds. Eur J Med chem. 2000;35:241-248.
14. Kalsi R, Shrimali M, Bhalla TN and Barthwal JP. Synthesis and anti-inflammatory activity of indolyi azetidinones. Indian J Pharm Sci. 2006;41;353-359.
15. Melnyk P, Leroux V, Sergheraert and Grellier P. Design, synthesis and invitro antimalarial activity of anacylhydrazone library. Biloorg Med chem left. 2006;16:31-35.
16. Patole J, Sandbhor U, Padhye S, Deobagkar DN, Anson CE and Powell A. Structuralchemistry and invitro anti tubercula activity of acetyl pyridine benzoyl hydrazone and its copper complex against Mycobacteriumsmegmatis. Bioorg Med Chem Lett. 2003;13:51-55.
17. Jaheer MD, Ranjith Reddy P, Narsimha N, Sujitha P, Srinivas B, Bhima B and Sarala Devi Ch. Synthesis, spectro-analytical, computational and biological studies of novel 6-methyl-3-(1-(4-oxo-2-phenylquinazolin-3(4H)-ylimino) ethyl)-2H-pyran-2, 4(3H)-dione and its Co (II), Cu (II) and Hg (II) metal complexes.IOSR Journal of Applied Chemistry. 2014;7:1-12.
18. Nisha aggarwal, Rajesh kumar, chitra srivastva, prem dureja and khuran JM. Synthesis of nalidixic acid based hydrazones as novel pesticides. J Agric Food Chem. 2010;58(5):3056-3061.

19. Padmaja A, Laxmi K and Sarala Devi Ch. Spectro-analytical studies on (E) - N'-(2 hydroxy benzylidene) benzohydrazide and its interaction with Cu (II). J Indian Chem Soc. 2011;88: 183-187.
20. Jeffrey C Pommerville, Jones and Bartlett Publishers Alcamo's laboratory Fundamentals of microbiology. 2005; Seventh edittion .
21. Zsolt Bikadi and Eszter Hazai. Aplication of thePM6 semi-empirical method to modeling to proteins enhances docking accuracy of Auto Dock. J cheminform. 2009;1:15.